Available online at www.sciencedirect.com

ScienceDirect

Proceedings of the Combustion Institute 37 (2019) 1919–1926

Proceedings of the Combustion Institute

www.elsevier.com/locate/proci

Premixed flame oscillations in obstructed channels with both ends open

Abdulafeez Adebiyi [a], Elizabeth Ridgeway [a], Rawan Alkandari [a], Amanda Cathreno [a], Damir Valiev [b], V'yacheslav Akkerman [a,*]

[a] *Center for Innovation in Gas Research and Utilization (CIGRU), Center for Alternative Fuels, Engines and Emissions (CAFEE), Computational Fluid Dynamics and Applied Multi-Physics Center, Department of Mechanical and Aerospace Engineering, West Virginia University, Morgantown, WV 26506, USA*

[b] *Center for Combustion Energy, Tsinghua University, Beijing 100084, China*

Received 1 December 2017; accepted 12 July 2018
Available online 4 August 2018

Abstract

An initially laminar premixed flame front accelerates extremely fast and may even trigger a detonation when propagating in a semi-open obstructed channel (one end of the channel is closed; the flame is ignited at the closed end and moves towards the open one). However, industrial and laboratory conduits oftentimes have both ends open, or vented, with a flame ignited at one of these ends. The latter constitutes the focus of the present work. Specifically, premixed flame propagation through a comb-shaped array of obstacles, in-built in a channel with both ends open, is studied by means of computational simulation of the reacting flow equations with fully-compressible hydrodynamics and an Arrhenius chemical kinetics. The parametric study includes various blockage ratios and spacing as well as the thermal expansion ratios, with oscillations of the burning rate observed in the majority of the cases, which conceptually differs from fast flame acceleration in semi-open channels. Such a difference is devoted to the fact that while the entire flame-generated jet-flow is pushed towards a single exit in a semi-open channel, in a channel with two ends open, this jet-flow is distributed between the upstream and downstream flows, thereby moderating flame propagation. The flame oscillations are nonlinear in all cases where they are observed. The oscillation period grows with the blockage ratio but decreases with the thermal expansion. The present results also support the recent experiments, modeling and theory of flames in obstructed channels with both ends open, which all yielded steady or quasi-steady flame propagation prior to the onset of flame acceleration. Indeed, the present oscillations can be treated as the fluctuations around a quasi-steady solution.

Keywords: Premixed flame; Obstructed channel; Flame oscillation; Computational simulation

I. Introduction

Premixed flames propagating in narrow channels may experience various behaviors such as oscillations [1], acceleration [2,3] or a sequence of

* Corresponding author.
E-mail address: Vyacheslav.Akkerman@mail.wvu.edu (V. Akkerman).

https://doi.org/10.1016/j.proci.2018.07.058
1540-7489

these trends [4]. In channels with smooth (unobstructed) walls, these effects are caused mainly by mechanistic boundary conditions such as nonslip walls. Specifically, a flame may accelerate in a channel with nonslip, adiabatic walls and one end open, when propagating from the closed end to the open one, because the entire new volume generated in the burning process is pushed towards the single exit in such a "semi-open" channel. In contrast, when both ends of a channel are open, the newly-generated volume is distributed between the upstream and downstream flows, towards both ends, which moderate the effect. Consequently, steady or quasi-steady flame propagation may occur instead of acceleration [1]. Other effects such as turbulence, thermal boundary conditions and non-equidiffusivity may also influence both the accelerative and oscillating trends [5–7].

It is nevertheless noted that flame acceleration in channels with adiabatic, nonslip walls is, actually, relatively moderate; moreover, the acceleration rate decreases with the channel width. This conceptually differs from the case of obstructed conduits, where a flame may accelerate enormously [8]. In fact, there was a general belief that turbulence is the major driver of flame acceleration in such an obstructed configuration [8–12] until Bychkov et al. [13,14] revealed a shockless, conceptually-laminar mechanism of extremely fast flame acceleration in semi-open channels or tubes with a comb-shaped array of tightly-packed obstacles. This acceleration is driven by delayed burning in the pockets between the obstacles, and it is equally strong for narrow and wide pipes, with turbulence playing only a supplementary role. While an optimal obstacles design was actively debated, a comb-shaped configuration yields fastest flame acceleration due to continuous feedback between the tip velocity and ignition in the new pockets [14]. Moreover, the tightly-packed obstacles provide a predictable acceleration mechanism, supported by an analytical model, which is opposed to the case of widely-spaced obstacles, when a chaotic turbulent motion plays a greater role and, consequently, leads to a higher uncertainty of the flame behavior. Since more predictable flame behavior is better for practical applications, such comb-shaped, tightly-packed obstacles are widely employed in the studies, including the present work.

However, industrial and laboratory applications on obstructed pipes oftentimes have both ends open, with ignition occurring at one of them. There is therefore a critical need to scrutinize premixed flame propagation in open obstructed pipes such as illustrated in Fig. 1. In particular, will the difference between the open and semi-open obstructed pipes be as paramount as that for unobstructed pipes? The latter question constitutes the focus of this work. Specifically, flame propagation through a comb-shaped array of obstacles in channels of various blockage ratios and widths, with both ends

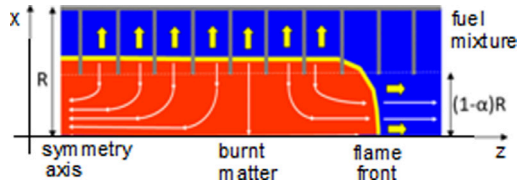

Fig 1. A schematic of an obstructed channel with both ends open, with the fuel mixture (blue), the burnt matter (red) and the flame front (orange line) between them. (For interpretation of the references to color in this figure legend, the reader is referred to the web version of this article.).

open, is studied by means of the computational simulations of combustion equations, with fully-compressible hydrodynamics and Arrhenius chemistry. As a result, we have identified regular oscillations of the burning rate in the majority of the simulation runs. These oscillations can be treated as fluctuations around a quasi-steady solution, being thereby in logical agreement with the modeling [15], experiments and in-situ modeling [16], and the analytical formulation [17], which all yielded near-steady flame propagation prior to the onset of flame acceleration in open obstructed channels. Such a transition to the acceleration trend is also observed in the present simulations, considering a wider channel and for a longer time. Moreover, the authors of [16] also reported cyclic oscillations of a discharge velocity in another experimental work [18]. On our part, we suspect that the oscillations are so quick, and presumably appear only at the initial stage of flame propagation, such that they are hard to be distinguished in the experiments. Overall, the present simulations agree with [15–18] but oppose extremely fast flame acceleration in semi-open obstructed channels [13,14]. Moreover, these results qualitatively reproduce the situation of *unobstructed* pipes, with acceleration in the semi-open channels [2] and oscillations in the open ones [1], both due to wall friction.

2. Description of numerical simulations

We have performed the computational simulations of the two-dimensional (2D) reacting flow equations, including fully compressible hydrodynamics, transport properties (heat conduction, diffusion and viscosity), and chemical kinetics represented by a single irreversible Arrhenius reaction of the first order, with the activation energy E_a and the constant of time dimension τ_R. More details of the numerical scheme and the entire solver can be found, for instance, in [1–4,14]. In particular, the basic equations read:

$$\frac{\partial}{\partial t}\rho+\frac{\partial}{\partial x_i}(\rho u_i)=0,\ \frac{\partial}{\partial t}(\rho u_i)+\frac{\partial}{\partial x_j}\left(\rho u_i u_j+\delta_{i,j}P\right)-\gamma_{i,j}=0, \quad (1)$$

$$\frac{\partial}{\partial t}\left(\rho\varepsilon+\frac{1}{2}\rho u_i u_j\right)+\frac{\partial}{\partial x_i}\times\left(\rho u_i h+\frac{1}{2}\rho u_i u_j u_j+q_i-u_j\gamma_{i,j}\right)=0, \quad (2)$$

$$\frac{\partial}{\partial t}(\rho Y)+\frac{\partial}{\partial x_i}\left(\rho u_i Y-\frac{\zeta}{Sc}\frac{\partial Y}{\partial x_i}\right)=-\frac{\rho Y}{\tau_R}\exp\left(-E_a/R_pT\right), \quad (3)$$

where Y is the mass fraction of the fuel mixture; $\varepsilon = QY + C_V T$ and $h = QY + C_P T$ the specific internal energy and enthalpy, respectively; $Q = C_P T_f(\Theta - 1)$ the energy release in the reaction, with the specific heats at constant volume, C_V, and pressure, C_P, the initial fuel temperature, $T_f = 300$ K, pressure, $P_f = 1$ bar, density $\rho_f = 1.16$ kg/m^3, and the thermal expansion ratio $\Theta \equiv \rho_f/\rho_b = T_b/T_f$ in the range $\Theta = 5 \sim 10$. The unstretched laminar flame speed is taken as $S_L = 3.47$ m/s, which resembles typical methane-air combustion. The speed of sound in this mixture is 100 times larger, $c_s = 347$ m/s, such that the hydrodynamics is almost incompressible at the initial stage of burning. Both the fuel mixture and burnt matter are assumed to be ideal gases of constant molecular weight, $M = 2.9$ kg/kmol, such that the equation of state is $P = \rho R_p T/M$, with the universal gas constant $R_p = 8.31\ kJ/(\text{kmol}\cdot\text{K})$. The stress tensor $\gamma_{i,j}$ and the energy diffusion vector q_i are given by

$$\gamma_{i,j} = \zeta\left(\frac{\partial u_i}{\partial x}+\frac{\partial u_j}{\partial x_i}-\frac{2}{3}\frac{\partial u_k}{\partial x_k}\delta_{i,j}\right),$$
$$q_i = -\zeta\left(\frac{C_p}{Pr}\frac{\partial T}{\partial x_i}+\frac{Q}{\text{Sc}}\frac{\partial Y}{\partial x_i}\right), \quad (4)$$

where $\zeta \equiv \rho\nu$ is the dynamic viscosity, being $\zeta_f = 1.7 \times 10^{-5}$ kg/(m · s) in the fuel mixture, and Pr and Sc are the Prandtl and Schmidt numbers, respectively. We took $\text{Pr} = \text{Sc} = 1$ such that the Lewis number was unity, $\text{Le} \equiv \text{Sc}/\text{Pr} = 1$. It is nevertheless recognized that flames are often nonequidiffusive ($\text{Le} \neq 1$) in practice, including the lean hydrogen mixtures considered in [15,16], and the impact of *Le* can be significant. In particular, faster propagation is expected for $\text{Le} < 1$ flames (due to the onset of the diffusional-thermal instability), whereas $\text{Le} > 1$ flames presumably propagate slower (due to extra flame thickening). However, in the present work we intentionally chose $\text{Le} = 1$ to eliminate the Le-effects, in particular, to avoid the diffusional-thermal instability. The Le-effects require a separate study that will be presented elsewhere.

The flame thickness is conventionally defined as $L_f \equiv \zeta_f/\rho_f S_L \text{Pr} = 4.22 \times 10^{-6}$ m. While the real width of the burning zone may exceed L_f by up to an order of magnitude [1], it is L_f that controls a Reynolds number associated with flame propagation, $\text{Re} \equiv RS_L/\nu = R/L_f\text{Pr} = R/L_f$, and an appropriate size of the computational grid. Specifically, the square cells of size $0.2\,L_f \times 0.2\,L_f$ were employed in the present simulations. The convergence of such a grid has been widely tested and discussed in the previous studies such as [13,14]. In the present work, we also made an extra resolution test using a standard procedure of [14]. Specifically, test simulation runs with different resolutions were performed and compared. The reaction zone was properly resolved at all times. The results showed convergence of the major characteristics such as the average burning rate and the oscillation period. The difference in average burning rates did not exceed 0.5%, while that in the oscillation periods did not exceed 6%.

A flame propagates in a long 2D channel of width $2R$, with both ends open, where the fraction $2R\alpha$ is blocked by the obstacles with a spacing (the distance between two neighboring obstacles) ΔZ. In this respect, the major dimensionless quantities of this study are the blockage ratio α, the scaled spacing $\Delta Z/R$, and the flame Reynolds number $\text{Re} = R/L_f$. To be specific, the following parameters were employed: $\text{Re} = 12;\ 36,\ \Theta = 5 \sim 10$, $\alpha = 1/3;\ 1/2;\ 2/3$, and $\Delta Z/R = 1/4;\ 1/2;\ 1$. One more dimensionless quantity to be considered is the instantaneous scaled burning rate U_w/S_L. Similar to [1,2], here we evaluate the latter value by means of the instantaneous scaled surface area (scaled length in 2D) of a corrugated flame front $U_w(t)/S_L \approx S_f(t)/2R$. The burning rate U_w calculated in such a manner correlates well with the flame displacement speed [2] and the consumption speed [19,20] as justified in [20].

The surface of the channel walls and obstacles is adiabatic, $\mathbf{n}\cdot\nabla T = 0$, and free-slip, $\mathbf{n}\cdot\mathbf{u} = 0$, where $\mathbf{n}$ is a normal vector at a wall/obstacle surface. Keeping in mind the symmetry of the problem, to save the computational time and memory, only a half of the channel was actually simulated, namely, that from the symmetry axis until the upper obstructed wall as illustrated in Fig. 1. The absorbing (non-reflecting) boundary conditions are employed at both opened ends to prevent the reflection of the sound waves and weak shocks. Similar to our previous study of flame oscillations in *unobstructed* channels [1], in the present work we employed the initial parameters of the fuel mixture in the laboratory reference frame: $\rho = \rho_f$, $T = T_f$, $u_z = -S_L$, while those at the burnt matter were: $\rho = \rho_f/\Theta$, $T = \Theta T_f$, $u_z = -\Theta S_L$. Obviously, such a distribution fulfills the matching conditions at the initially planar flame front and would provide steady flame propagation as long as its shape was planar and the velocity field would balance the burning velocity. However, the flame will immediately get corrugated due to a non-uniform flow velocity profile across the unobstructed part of the channel such that the

flame surface area will exceed that of the planar flame. Consequently, the total instantaneous flame velocity with respect to the fuel mixture exceeds S_L such that the reaction zone moves towards the right end. The initial flame structure was imitated by the classical Zeldovich–Frank–Kamenetsky (ZFK) solution for a planar flame front [21] initiated at a distance $50\,L_f$ from the left (burnt) end of the channel.

3. Results

We investigated premixed flame propagation and the flame-generated flow velocity fields in obstructed channels with both ends open. An initially planar ZFK flame (not shown in the figures) acquires promptly a curved shape. It is observed that the length and curvature of the flame front vary as the flame propagates. Specifically, the variations of the scaled burning rate U_w/S_L show that the flame front oscillates in a periodic manner. As a result, we have analyzed the flame dynamics and morphology and the evolution of the velocity field during the oscillation.

The color temperature snapshots of Fig. 2 show the evolution of the flame front for $\alpha = 1/3$, Fig. 2a, $\alpha = 1/2$, Fig. 2b, and $\alpha = 2/3$, Fig. 2c, respectively. In all three cases $\Delta Z = R/4$ and $\Theta = 8$ such that the temperature varies from 300 K in the fresh fuel mixture (blue) till 2400 K in the burnt gas (red). To better illustrate the flow evolution and the flame structure in the cavities, we also present the zoomed version of the snapshots (ii)

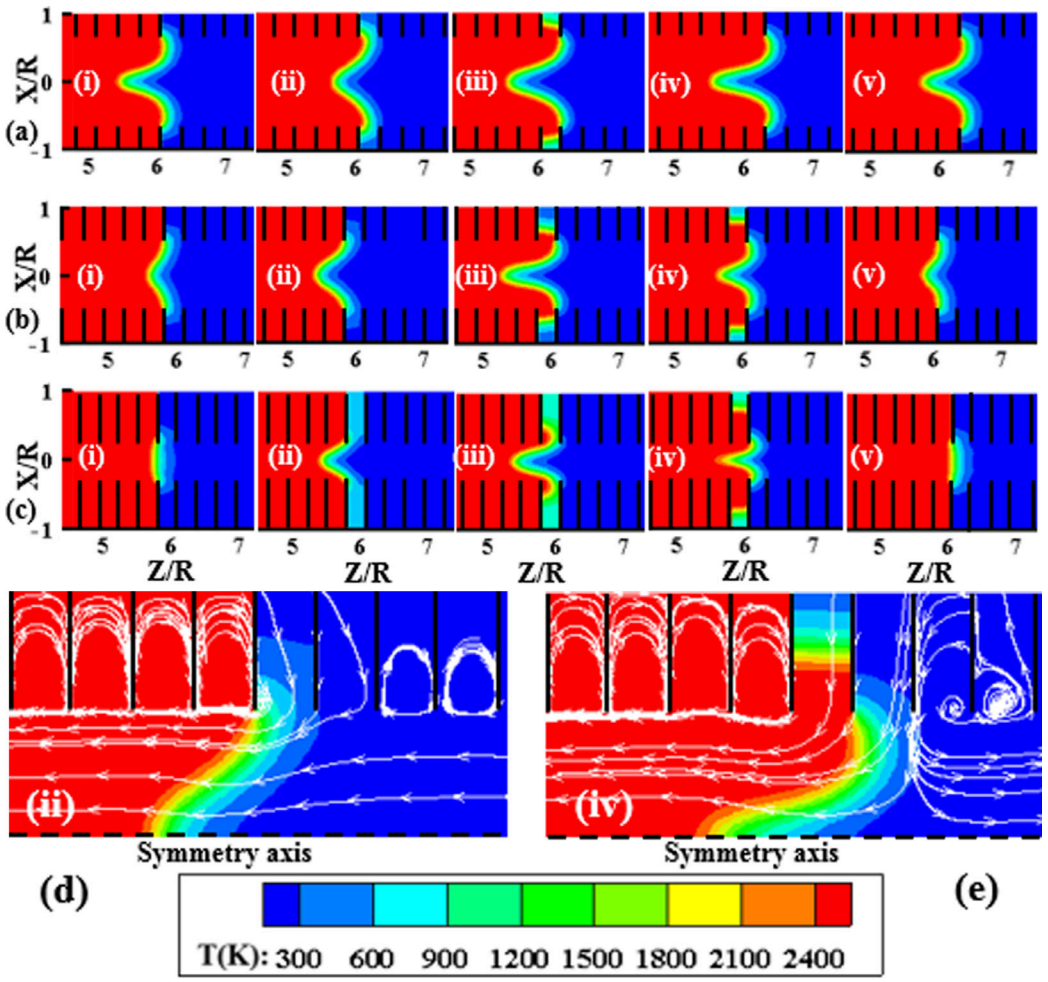

Fig 2. Consecutive color temperature snapshots and the flow streamlines (white) for the propagation of a flame with the thermal expansion ratio $\Theta = 8$ in a channel with the obstacle spacing $\Delta Z = R/4$ and various blockage ratios: $\alpha = 1/3$ (a), 1/2 (b), and 2/3 (c). Figures (d) and (e) are the zoomed versions of the snapshots (ii) and (iv) for $\alpha = 1/2$ provided to illustrate the processes in the cavities and to recall that only a half of a channel was simulated.

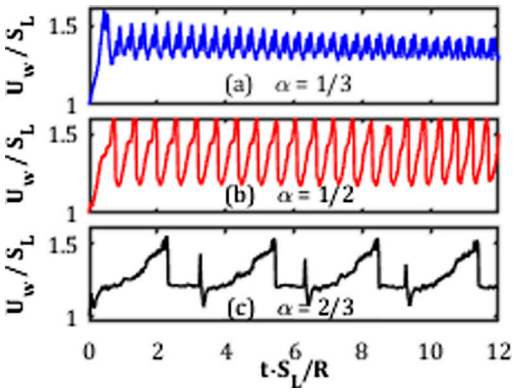

Fig. 3. The scaled burning rate U_w/S_L versus the scaled time tS_L/R for the thermal expansion ratio $\Theta = 8$, the obstacle spacing $\Delta Z/R = 1/4$, and various blockage ratios: $\alpha = 1/3$ (a), 1/2 (b), and 2/3 (c).

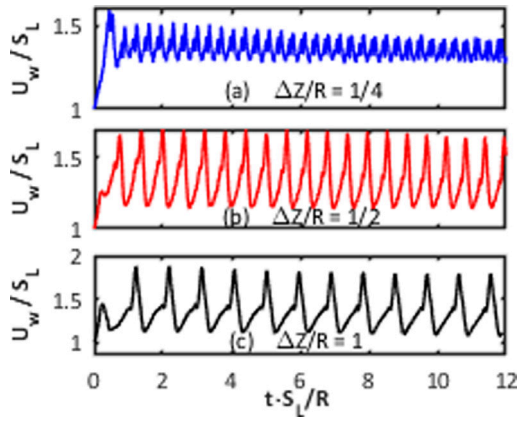

Fig. 4. The scaled burning rate U_w/S_L versus the scaled time tS_L/R for the thermal expansion ratio $\Theta = 8$, the blockage ratio $\alpha = 1/3$ and various obstacle spacing: $\Delta Z/R = 1/4$ (a), 1/2 (b) and 1 (c).

and (iv) for $\alpha = 1/2$ in Fig. 2d and e, respectively. The flow streamlines are shown in white. A flame segment in the free (unobstructed) part of the channel generally acquires a concave shape, with a formation of a cusp directed towards the burnt gas at the centerline. The other flame segments enter the pocket between the obstacles. We also recall that only the upper half of a channel was actually simulated as depicted in Figs. 1, 2e and d. Fig. 2(a–c) present the entire width of a channel for illustrative purposes only.

At the initial stage of each oscillation, a flame is almost quiescent as shown by the snapshots (i)–(ii) in all the figures. The duration of such a stationary stage increases with α, whereas the concavity of the flame front is smaller for larger α. During this stage, a flame starts consuming the fuel mixture in the pocket; the burning gas expands, and a newly-generated gas volume bends a flame segment in the pocket, making it convex, while that near the centerline remains concave; see also Fig. 2d. Consequently, the cumulative surface area (length) of the flame front grows, thereby promoting the total burning rate and yielding flame acceleration at this stage. However, as burning proceeds in a pocket, the flame eventually enters the next pocket and its front gets broken by the obstacle; see also Fig. 2e. Such a breaking of the flame front terminates acceleration, so the flame decelerates, as shown by snapshots (iii)–(iv) in Fig. 2(a–c), until the shape (v) of Fig. 2(a and b) is acquired. The acceleration–deceleration scenario described above repeats on a regular basis thus yielding flame oscillations. As a result, a flame propagating in the pockets between the obstacles experiences several stages of burning, during which the instantaneous flame shape, length and velocity substantially vary, thus exhibiting not a steady state but the oscillations. However, these oscillations are identical as long as the obstacles are identical as well as the pockets between them.

To quantify the oscillations, we plotted the evolution of the scaled instantaneous burning rate, U_w/S_L, for various α, ΔZ and Θ. In particular, Fig. 3 scrutinizes the impact of the blockage ratio on the burning rate oscillations by comparing the cases of $\alpha = 1/3,\ 1/2,\ 2/3$ (Figs. 3a–c, respectively), with fixed $\Delta Z = R/4$ and $\Theta = 8$. It is seen that the oscillations are nonlinear, and this nonlinearity is stronger for larger α. In the $\alpha = 1/3$ channel, a secondary peak appears for each oscillation.

Overall, there are three basic quantities characterizing the flame oscillations: the oscillation period τ_p, the oscillation amplitude ΔU, which slowly dampens with time in Fig. 3, and the average burning rate during an oscillation $\langle U_w \rangle$. According to Fig. 3, τ_p increases with α such that the largest period, with the most profound nonlinearity, is seen for $\alpha = 2/3$. The latter effect can be attributed to the fact that the larger blockage ratios correspond to the deeper pockets and thereby longer duration of a near-quiescent stage observed. The role of ΔZ is described by Fig. 4, where the cases of $\Delta Z = R/4$, Fig. 4a, $\Delta Z = R/2$, Fig. 4b, and $\Delta Z = R$, Fig. 4c, are compared for the fixed $\alpha = 1/3$ and $\Theta = 8$. The effect of spacing is found to be noticeable. In particular, both the oscillation period and nonlinearity get promoted with the increase in $\Delta Z/R$.

Finally, we investigated the influence of thermal expansion of the burning matter on the flame oscillations by varying the expansion ratio in the range $\Theta = 5 \sim 10$. Specifically, Fig. 5 compares the evolutions of the burning rate for $\Theta = 5$, Fig. 5a, $\Theta = 8$, Fig. 5b, and $\Theta = 10$, Fig. 5c, with the same $\Delta Z = R/4$ and $\alpha = 1/3$ in all three cases. It is clearly seen that the oscillation period reduces and nonlinearity weakens with Θ,. Indeed, instead of regular and smooth oscillations for $\Theta = 10$ in Fig. 5c, we see strong nonlinearity and irregularity for $\Theta = 5$ in Fig. 5a. Figures 6 and 7 are the counter-

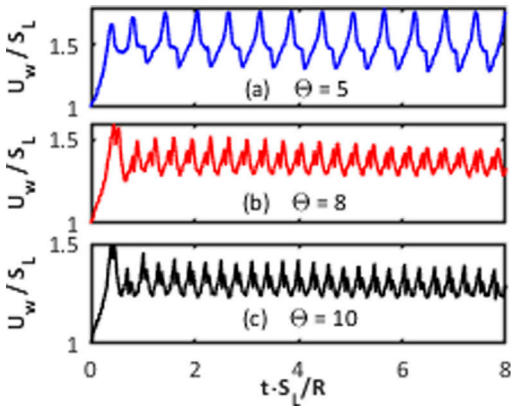

Fig. 5. The scaled burning rate U_w/S_L versus the scaled time tS_L/R for the blockage ratio $\alpha = 1/3$, the obstacle spacing $\Delta Z = R/4$ and various thermal expansion ratios: $\Theta = 5$(a), $\Theta = 8$(b), $\Theta = 10$ (c).

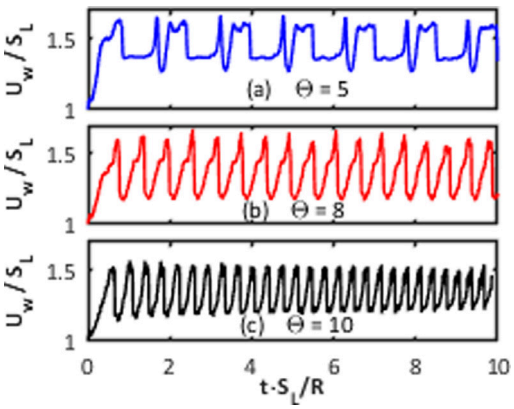

Fig. 6. The scaled burning rate U_w/S_L versus the scaled time tS_L/R for the blockage ratio $\alpha = 1/2$, the obstacle spacing $\Delta Z/R = 1/4$ and various thermal expansion ratios: $\Theta = 5$ (a), $\Theta = 8$ (b), and $\Theta = 10$ (c).

parts of Fig. 5 for $\alpha = 1/2$ (Fig. 6) and $\alpha = 2/3$ (Fig. 7), respectively. In fact, all three figures yield the same conclusion: the reduction in Θ promotes both nonlinearity and the oscillation period τ_p. At the same time, nonlinearity itself is much stronger in Figs. 6 and 7 as compared to Fig. 5. The latter is obviously devoted to the larger α.

To quantify the qualitative conclusions of Figs. 5–7, we also plotted the scaled oscillation period $\tau_p S_L/R$, the scaled average burning rate $\langle U_w \rangle/S_L$, and the scaled oscillation amplitude $\Delta U/S_L$ versus the thermal expansion ratio Θ; see Fig. 8a, b, and c, respectively. Specifically, Fig. 8a shows that τ_p reduces with Θ for any blockage ratio, but the effect is minor for $\alpha = 1/3$ and it is quite moderate for $\alpha = 1/2$. In contrast, the reduction in τ_p is dramatic for $\alpha = 2/3$. The average burning rate $\langle U_w \rangle$, Fig. 8b, also reduces with Θ for any α, but here the situation is qualitatively different from Fig. 8a: the effect appears minor for a large blockage ratio, $\alpha = 2/3$, but it is noticeable for the smaller α. As for the oscillation amplitude ΔU, Fig. 8c, it reduces with Θ as long as the blockage ratio is moderate, $\alpha = 1/3$, while for larger α the Θ-dependence of ΔU is non-monotonic.

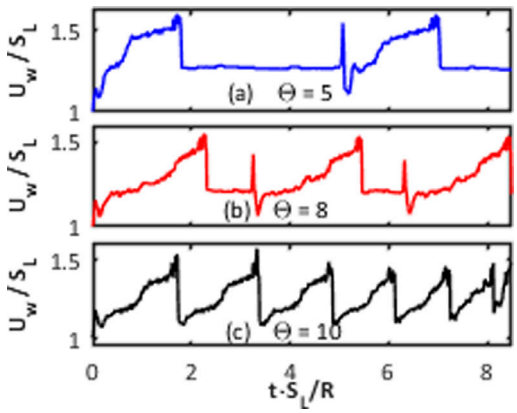

Fig. 7. The scaled burning rate U_w/S_L versus the scaled time tS_L/R for the blockage ratio $\alpha = 2/3$, the obstacle spacing $\Delta Z/R = 1/4$ and various thermal expansion ratios: $\Theta = 5$ (a), $\Theta = 8$ (b), and $\Theta = 10$ (c).

4. Summary and discussion

In this work, we identified and scrutinized premixed flame oscillations in 2D obstructed channels, with both ends open, by means of the computational simulations. Specifically, the oscillations in the channels of half-width $R/L_f = \mathrm{Re} = 12$ with the blockages ratios $\alpha = 1/3$, $1/2$, $2/3$ and the obstacles spacing $\Delta Z/R = 1/4$; $1/2$; 1 were analyzed. The flame evolution is illustrated by the color temperature snapshots of Fig. 2, while the burning rate is quantified versus time in Figs. 3–7. The oscillations of the burning rate are characterized by the oscillation period, τ_p, amplitude, ΔU, and the average burning rate $\langle U_w \rangle$. The latter three quantities are presented versus the thermal expansion ratio Θ in Fig. 8. It is shown that Θ and α influence the oscillations both qualitatively and quantitatively. Overall, the oscillations differ conceptually from ultrafast flame acceleration in semi-open obstructed channels [13,14], but they resemble the oscillations found in unobstructed channels with both ends open [1]. Moreover, treated as fluctuations around steady flame propagation, the oscillations agree with the modeling [15,16], experiments [16,18], and theory [17] of flames in channels with both ends open (or vented) in terms that all of the studies [15–18] identified steady flame propagation prior to fast acceleration. Such agreement between our work and [15–17] is also illustrated by Fig. 9,

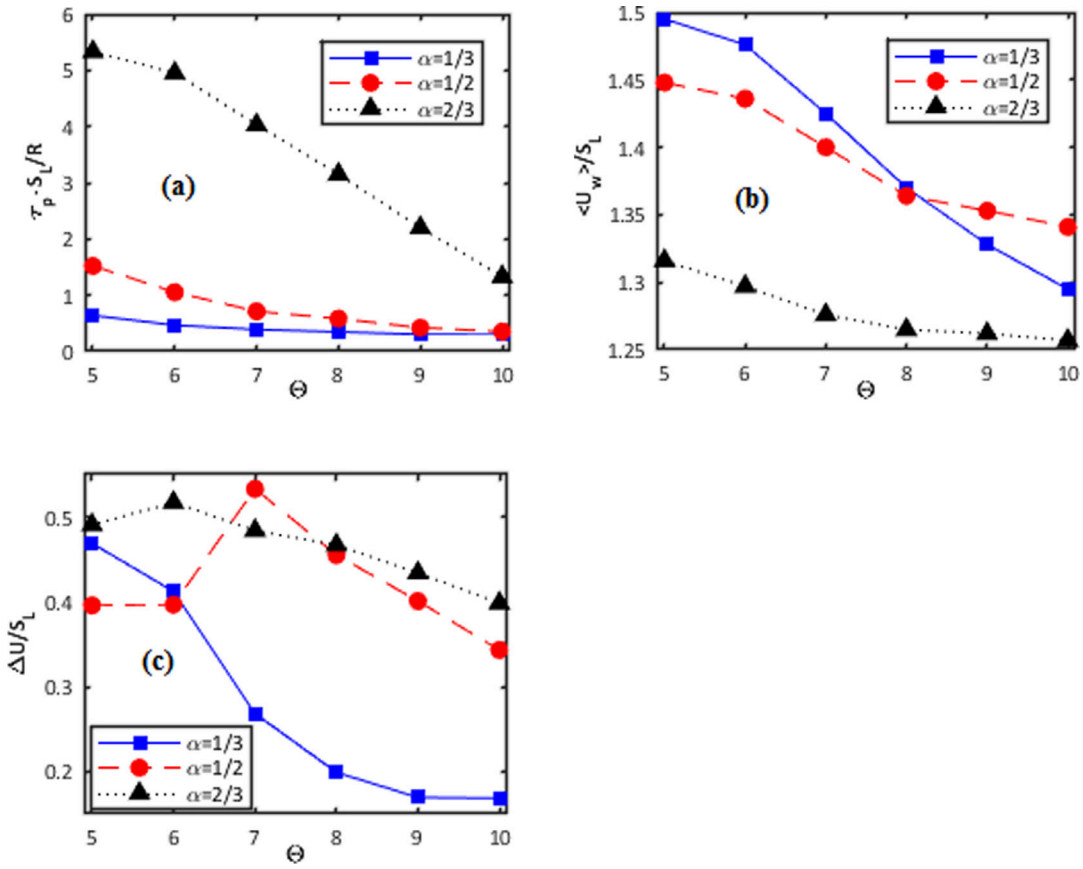

Fig. 8. The scaled oscillation period $\tau_p S_L/R$ (a), the average burning rate during an oscillation $\langle U_w \rangle/S_L$ (b), and the scaled oscillation amplitude $\Delta U/S_L$ (c) versus the thermal expansion ratio Θ for the obstacles spacing $\Delta Z/R = 1/4$ and various blockage ratios: $\alpha = 1/3;\ 1/2;\ 2/3$.

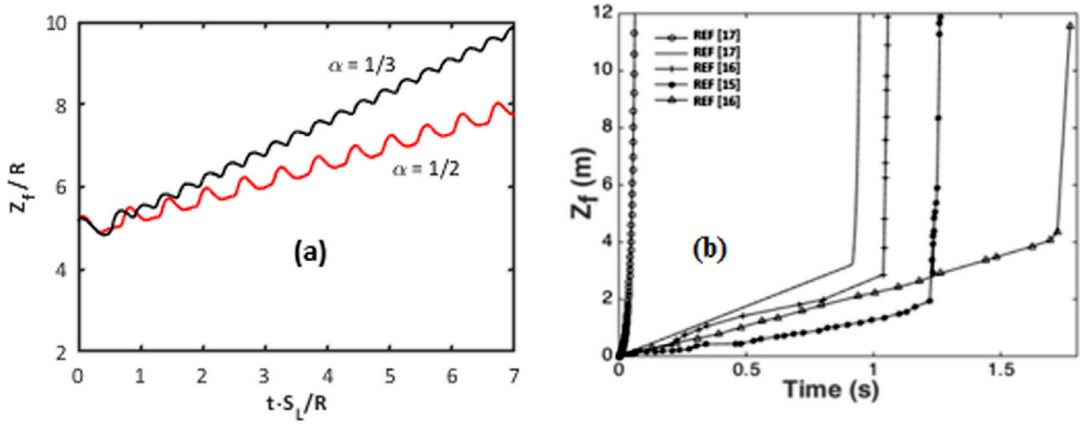

Fig. 9. Qualitative comparison of quasi-steady flame propagation (oscillations) in the present work (a) and steady flame propagation at the initial stage (prior to sudden acceleration) [17] (b).

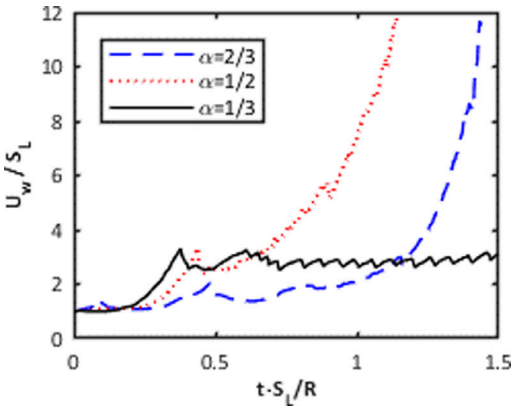

Fig. 10. The scaled burning rate U_w/S_L versus the scaled time tS_L/R for Re = 36, $\Theta = 8$, $\Delta Z/R = 1/4$ and various blockage ratios: $\alpha = 1/3$ (solid), 1/2 (dotted), and 2/3 (dashed).

where quasi-steady flame propagation (oscillations) of the present work, Fig. 9a, is compared to steady flame propagation at the initial stage of burning [15–17], Fig. 9b.

Finally, while the oscillations discussed above were obtained in a relatively narrow channel, Re = 12, we also performed a pilot set of simulations for a wider channel, Re = 36. The result is shown in Fig. 10, where the time evolution of the scaled burning rate U_w/S_L is plotted for $\alpha = 1/3$ (solid), $\alpha = 1/2$ (dotted) and $\alpha = 2/3$ (dashed). It is seen that the initial oscillations are eventually replaced by sudden and prompt acceleration for $\alpha = 1/2$ and $\alpha = 2/3$, while this is not the case for a smaller blockage ratio, $\alpha = 1/3$. In fact, we may suspect that a transition from oscillations to acceleration may require more time for narrower channels and smaller α such that the transition is observed only in some of the simulation runs reported here. Obviously, such a transition in Fig. 10 resembles that in Fig. 9b. In addition, being conceptually different from ultrafast flame acceleration in semi-open obstructed channels [13,14], the flame oscillations revealed in the present work actually resemble the oscillations found in *unobstructed* channels with both ends open [1]. Consequently, the present study agrees with [1,15–17].

Acknowledgments

This study was sponsored by the U.S. National Science Foundation (NSF) through the CAREER Award #1554254 (V.A.) as well as by the West Virginia Higher Education Policy Commission through the grant #HEPC.dsr.18.7 (V.A.).

References

[1] V. Akkerman, V. Bychkov, A. Petchenko, L.-E. Eriksson, *Combust. Flame* 145 (2006) 675.
[2] V. Bychkov, A. Petchenko, V. Akkerman, L.-E. Eriksson, *Phys. Rev. E* 72 (2005) 046307.
[3] V. Akkerman, V. Bychkov, A. Petchenko, L.-E. Eriksson, *Combust. Flame* 145 (2006) 206.
[4] V. Akkerman, C.K. Law, V. Bychkov, L.-E. Eriksson, *Phys. Fluids* 22 (2010) 053606.
[5] E.S. Oran, V. Gamezo, *Combust. Flame* 148 (2007) 4.
[6] G. Pizza, C.E. Frouzakis, J. Mantzaras, A.G. Tomboulides, K. Boulouchos, *Combust. Flame* 152 (2008) 433.
[7] C. Cui, M. Matalon, T.L. Jackson, *AIAA J.* 43 (2005) 1284.
[8] G. Roy, S. Frolov, A. Borisov, D. Netzer, *Prog. Energy Combust. Sci.* 30 (2004) 545.
[9] G. Ciccarelli, C. Fowler, M. Bardon, *Shock Waves* 14 (2005) 161.
[10] M. Kuznetsov, V. Alekseev, I. Matsukov, S. Dorofeev, *Shock Waves* 14 (2005) 205.
[11] G. Ciccarelli, S. Dorofeev, *Prog. Energy Combust. Sci.* 34 (2008) 499.
[12] V. Gamezo, T. Ogawa, E. Oran, *Combust. Flame* 155 (2008) 302.
[13] V. Bychkov, D. Valiev, L.-E. Eriksson, *Phys. Rev. Lett.* 101 (2008) 164501.
[14] D. Valiev, V. Bychkov, V. Akkerman, C.K. Law, L.-E. Eriksson, *Combust. Flame* 157 (2010) 1012.
[15] P. Middha, O.R. Hansen, *Proc. Saf. Prog.* 27 (2008) 192.
[16] J. Yanez, M. Kuznetsov, V. Bykov, in: 24th international colloquium on the dynamics of explosions and reactive systems, Taipei, Taiwan, July 28–August, 2, 2013, pp. 1–6.
[17] V. Bychkov, J. Sadek, V. Akkerman, *Phys. Rev. E* 95 (2017) 013111.
[18] J. Yanez, M. Kuznetsov, V. Bykov, "Sudden acceleration of flames in open channels driven by hydraulic resistance," https://arxiv.org/pdf/1208.6453.pdf
[19] A. Petchenko, V. Bychkov, V. Akkerman, L.-E. Eriksson, *Combust. Flame* 149 (2007) 418.
[20] V. Akkerman, V. Bychkov, L.-E. Eriksson, *Combust. Flame* 151 (2007) 452.
[21] Ya.B. Zeldovich, G.I. Barenblatt, V. Librovich, G. Makhviladze, *Mathematical Theory of Combustion and Explosions*, Consultants Bureau, New York, 1985.